



## KINETIC EFFECT ON FLEXIBLE BODIES BEHAVIOR

Eduardo BOTERO<sup>1</sup> and Miguel P. ROMO<sup>2</sup>

### SUMMARY

When a flexible body starts sliding due to earthquake shaking, it acquires kinetic energy that coupled with the seismic forces modifies its base-fixed behavior. One of the reasons why this happens is that the excitation motions are modified when sliding of the body occurs.

In this paper a numerical method that considers coupling between the sliding flexible body and the surface on which it slides is advanced. Also, a one-axial shaking table that allows simulation of the phenomena is briefly described using a physical model instrumented with accelerometers and a linear variation displacement transducer. The response of the sliding body is recorded and the information used to study the change in the behavior of a fixed-base flexible structure when its sliding is allowed.

A number of test conditions were considered in this research, but only the influence of the sliding on the response of the flexible body is reported in this paper. Basically, the effect of input motion characteristics and the flexibility of the sliding body are investigated herein.

### INTRODUCTION

Over the past, it has been a common practice to compute earthquake-induced permanent displacements in slopes, resorting to the so called rigid-block approach (i.e., Newmark [1] and Ambraseys [2]). However, during the past twenty years or so, some improvements have introduced to this method although the main hypotheses have remained unchanged. Accordingly the flexibility of the sliding mass has replaced the rigid-mass assumption, allowing the motion vertical variation to be accounted for the analyses (i.e., Makdisi [3], Chopra [4]). More recently, the procedures have been modified to include additionally the potential effects of the inertia acquired by the soils mass when sliding (i.e., Kramer [5], Rathje [6], Botero [7], [8] and [9]). Much of the research on this theme has been oriented to evaluate the effects of the body flexibility and inertia of the sliding mass on permanent displacements, comparing (mostly) theoretical results obtained from analytical studies with the values obtained (also mostly analytical) applying a rigid block approach. Thus, it has been learnt what the potential influence might be of these two factors on the sliding characteristics evaluated by rigid-block procedures.

<sup>1</sup> PhD. Student, Institute of Engineering, National University of Mexico

<sup>2</sup> Head Research, Institute of Engineering, National University of Mexico

Although many advances have been made in the comprehension of this phenomenon, it is believed that there is no clear understanding as to how the inertia of the sliding mass influences the vibration characteristics of a given body. In other words, knowing the vibration modes and resonant frequencies of a base flexible body, how these would be modified by its sliding, i.e., free-base flexible body?

To this end, a discrete model like the one shown in Figure 1 was placed on a horizontal shaking table and its response measured under fixed-base and free-to-slide conditions. The main results and pertinent discussions are included in this paper. Furthermore, the results of these tests are used to evaluate the predicting capabilities of an analytical model recently developed by the authors Botero and Romo [7].

## LABORATORY TESTS

A one dimensional shaking table was built to perform the laboratory tests. It uses a pneumatic actuator to generate the excitation and the shaking table hardware is controlled by a computer. The shaking table instrumentation consists of four three-axial accelerometers and one linear variation displacement transducers.

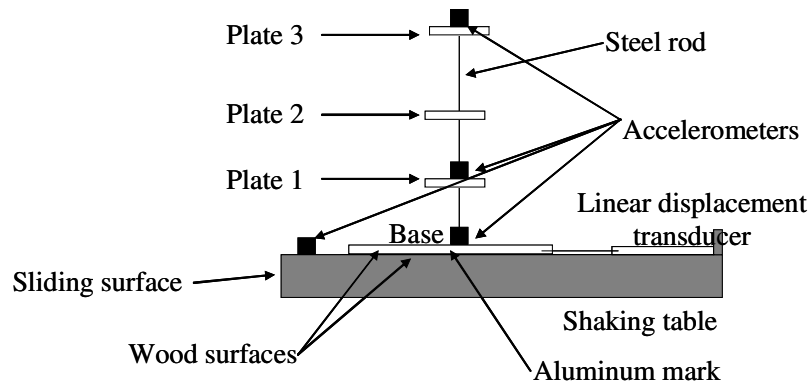


Figure 1. Schematic flexible model representation

The model (Figure 1), implemented for the analysis, consists of a rigid base that is constituted by a wooden table and aluminum frame, the upper mass of the model is distributed in three circular plates, which are connected by two flexible steel rods that are fixed to the model base. In the results presented herein the model was excited with a sine wave lasting 32 sec and having a 1.4 Hz-constant frequency. The sliding platform of the table was kept horizontal in all tests. The response of the model was monitored by installing one accelerometer right below the interface, other at the model base (just above the interface) and the other two on the one and three plates, respectively.

## MATHEMATICAL MODEL

### Equilibrium equation

For rigid bodies (Figure 2) the acting forces are only the resistant force ( $F_r$ ), given by the normal force ( $N$ ) times the static friction coefficient and the acting force ( $F_a$ ) induced by the external excitation.

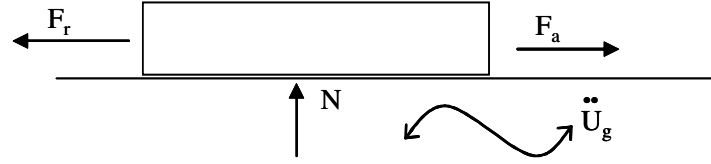


Figure 2. Acting forces on the rigid model

The forces induced in the flexible body (Figure 3) by the forces acting upon the model depend on the weight of the body, the mass distribution, the stiffness and damping properties of the different constitutive materials (rods and plates), and the resulting inertia forces.

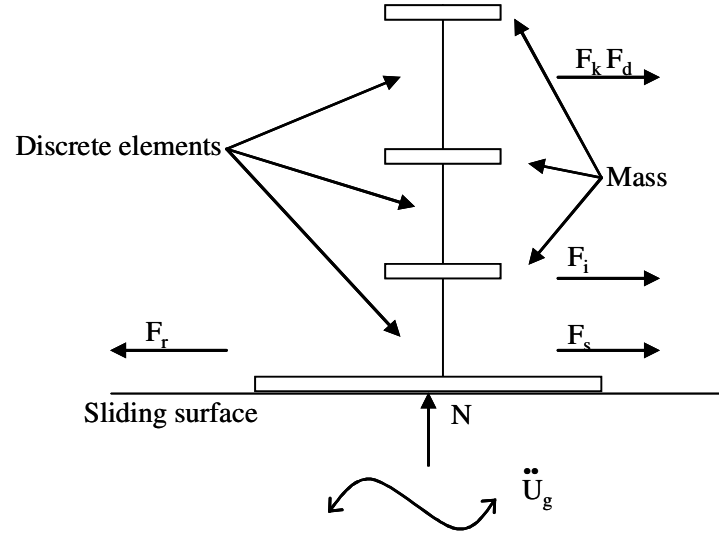


Figure 3. Acting forces on the flexible sliding body

The acting forces on the flexible model are show in figure 3. The resistant force  $F_r$ , is given by the weight of the model times the friction coefficient. If should be realized that the friction coefficient changes from a static stage to a dynamic one, when sliding at the interface occurs. On the other hand, the unbalancing forces are caused by the inertia of the model masses caused by both the input motion and the sliding of the model. The driving force (Equation 1) results from the active forces in the system, which is given by (i.e., Botero [10]):

$$F_a = F_s + F_k + F_d + F_i \quad (1)$$

Where  $F_s$  is the shear force at the model base due to the overlying weight;  $F_k$  is the stiffness force due to the relative displacement between consecutive nodes,  $F_d$  is the damping force due to the relative velocity between neighboring nodes and  $F_i$  is the inertia force caused by the mass of plate  $i$  times the total acceleration (including the sliding effects). The driving force can be expressed as:

$$F_a = M_1 g \sin(\theta) + kU + c\dot{U} - m_b \left( \ddot{U}_g + \ddot{U}_0 \right) \quad (2)$$

Where  $M_1$  is the total mass, which is given by the addition of all masses of the system,  $g$  is the gravity force,  $\theta$  is the inclination of the sliding surface,  $k$  is the element stiffness,  $U$  is the relative displacement of consecutive nodes;  $c$  is the element damping,  $\dot{U}$  is the relative velocity between neighboring nodes;

mass  $m_b$  is the mass directly over the sliding surface,  $\ddot{U}_0$  is the kinetic acceleration of the system and  $\ddot{U}_g$  the external acceleration.

During seismic excitation, the body can remain in equilibrium through long periods of time, but the force equilibrium in the sliding surface may be broken and then  $F_a > F_r$  leading to permanent displacements, until the driving force drops below the resisting force. Then, the ground velocity and the system velocity are equal and the kinetic acceleration is equal to zero.

### Movement equation

The response of each node, when the system does not slide, can be computed with the following equation of motion:

$$[M]\left(\ddot{U}\right)+[c]\left(\dot{U}\right)+[k]\left(U\right)=-M_1\left(\ddot{U}_g \cos(\theta)\right) \quad (3)$$

Where  $M$  is the mass matrix formed with the concentrated masses of the discrete system above the sliding surface,  $\ddot{U}$  is the relative acceleration vector. When the system slides, force equilibrium at the interface defines the kinetic acceleration. The equation of motion for this condition is given by:

$$[M]\left(\ddot{U}\right)+[c]\left(\dot{U}\right)+[k]\left(U\right)=-M_1\left(\ddot{U}_c+\ddot{U}_g \cos(\theta)\right) \quad (4)$$

Where  $\ddot{U}_c$  is the kinetic acceleration (for more details as to how this function is obtained see Botero and Romo ([8], [9], [10] and [11])

### STUDY CASE

The flexible body is a uniformly-distributed lumped-mass model (Figure 4). The base friction parameters (static and dynamic) of the free-to-slide model are assumed equal and the model weight of both models (fixed-base and free-to-slide) are equal. The model's characteristics and material properties are similar in both cases. The sliding plane was always horizontal, so the free-to-move model moved back and forth when the yield acceleration was exceeded.

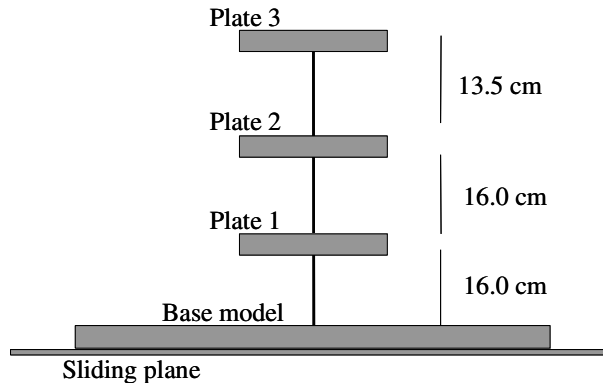


Figure 4. Laboratory model

The accelerations registered by the accelerometers located on the base of both models, on plates 1 and 3, and over the sliding plane are shown in figure 5. Two tests were performed. In one, the flexible model was fixed to the sliding plane and the model remained “welded” all time during the test. In the second test, the model was free-to-displace over the sliding surface.

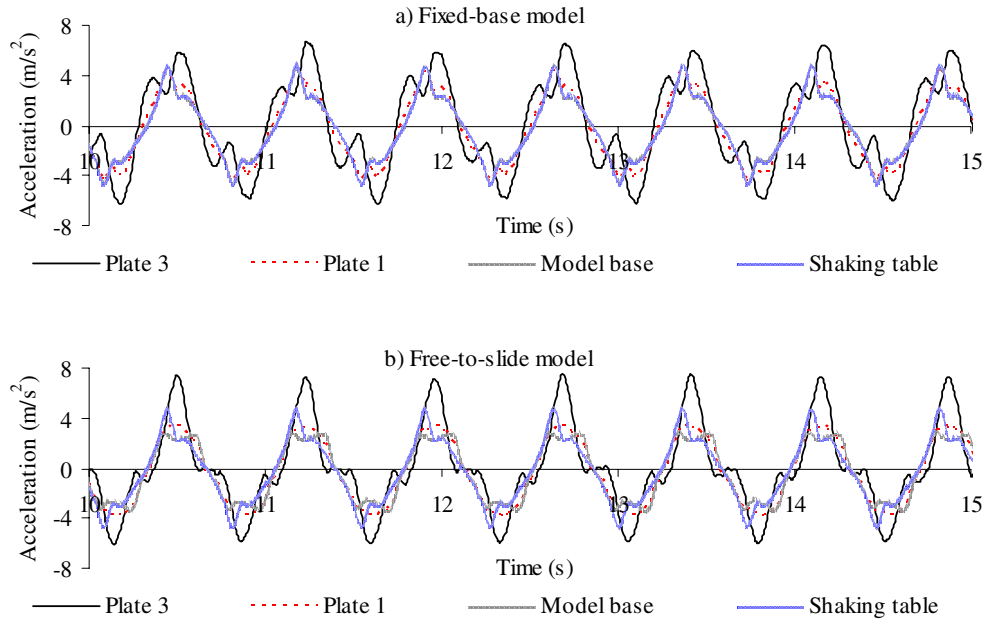


Figure 5. Resultant accelerations in the flexible model

The responses of both models are shown in Figure 5. The input motion (provided by the shaking table) is the same. The records obtained at various locations of the lumped mass models clearly indicate that the vibration characteristics are different, mainly on account on the model base boundary conditions.

The fixed-base model response indicates that since its base remains in contact (welded) to the shaking table, their motions are identical. Plate 1 motions are slightly different to the input, indicating that the steel rod that links this lumped mass with the base model is rather stiff. However, some amplification is noticeable. The influence of the flexibility of the model is more notorious in the recorded response of plate 3. The accelerogram shows that the motion is still periodic (as is the excitation). However, a double-peak response is generated because the overall flexibility of the model.

The vibration characteristics of the free-to-slide model are completely modified from the model base above, once sliding develops. Figure 5b shows that the yield acceleration in this case is around  $3.2 \text{ m/s}^2$ , which remained almost constant during few seconds and then dropped until the input acceleration reversed its direction and again exceeded the yield acceleration forcing the model to displace back. This pattern repeats itself during the whole excitation. From the base level up, the responses of the lumped masses are different to those of the fixed-base model.

With the purpose of appreciating in more detail the effects of the free-to-slide base model on the overall response of the lumped mass, in Figure 6 the responses of each component of the model are compared. Figure 6 shows that the input motion for both models are identical, thus ensuring that the observed differences are due exclusively to the base boundary conditions. The results of Figure 6c show that when the yield acceleration is reached the free-to-slide model starts accumulating displacements, while the

fixed-base model transmits the motions as depicted by the recorded movements. It is interesting to notice that when the base of the free-to-slide model starts moving, the yield acceleration decreases during few seconds to begin increasing again up to reach a maximum value from which the acceleration decreases quickly, drops to zero and reverses its direction until the yield acceleration is reached and the sliding phenomenon develops again, but in the opposite sense. This phenomenon repeats itself while the excitation lasts.

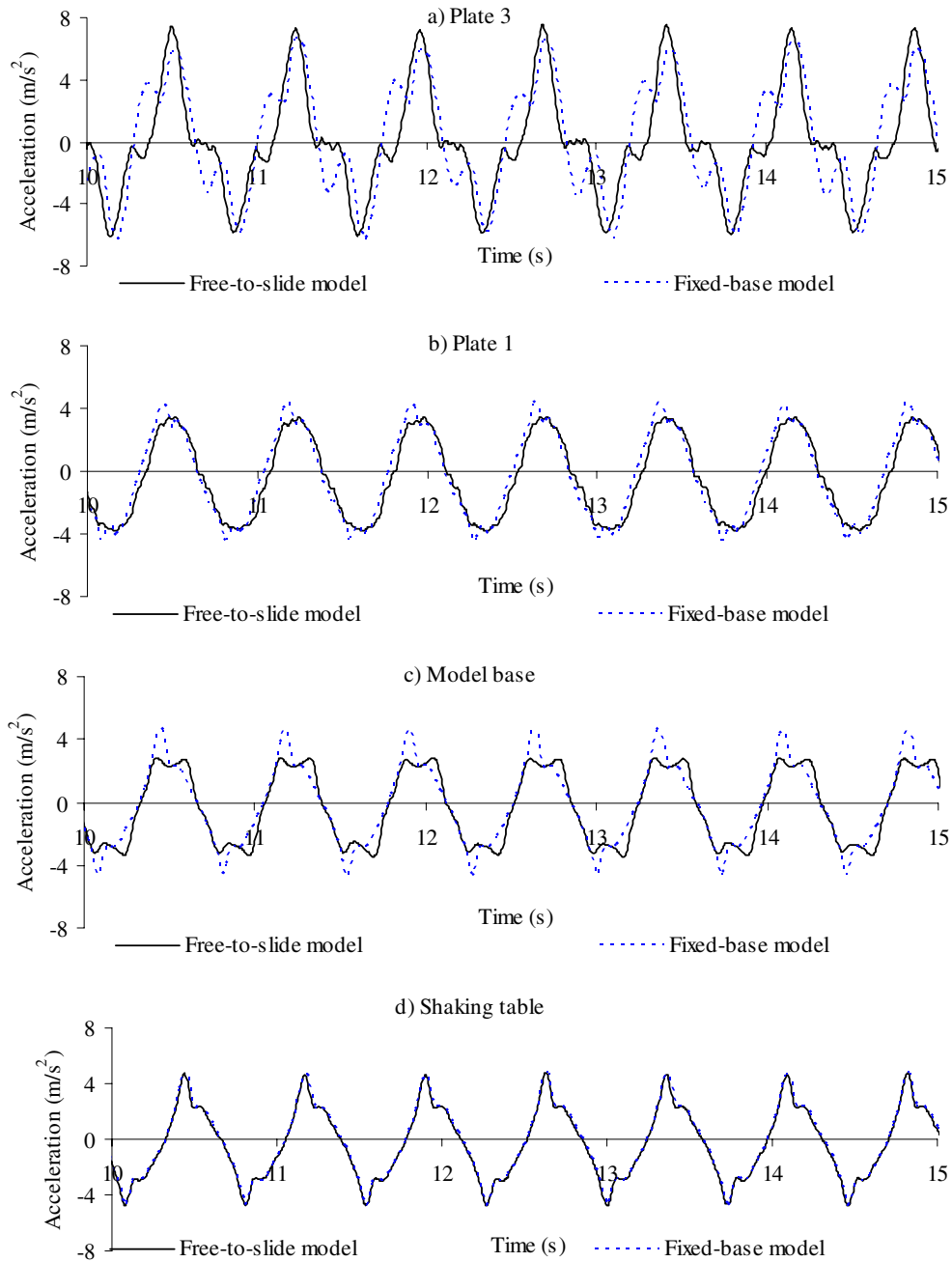


Figure 6. Resulting accelerations in the coupled and decoupled tests

From the model base level up, the responses of both models begin to branch of. It would seem that actual excitation in the free-to-slide model is defined by the vibration characteristics of the motions developed at the model base-shaking table interface. None-the-less, both models amplify the accelerations, although the pattern of the resulting accelerograms differs perceptibly.

Finally, it is worth noticing that when the model slides, the input motion is only partially transmitted to the model. This fact questions the common hypothesis, which implies that the full input motion acts upon the sliding body. Henceforth, it can be concluded that some energy of the input motion dissipates (probably by heat) at the interface. This aspect has been recognized previously by Houston [12], who suggested that the motions used to compute earthquake-induced displacements in slopes should be reduced about 25%. Although this is a step forward, as it will be seen later, the amount of energy dissipation varies during the time period the sliding of the body lasts.

Another aspect that needs to be highlighted is related with the response of plate 3 for both models. When the base is fixed, the accelerogram has a double-peak possibly due to the effect of the two vibration modes. On the other hand, the case of free-to-slide model, the accelerogram depicts only one peak. This is likely due to sliding of the body that masks the effect of the second vibration mode. However, comparing the accelerograms, it is realized that the amplitude of the maximum acceleration is higher in the latter case. It may be argued that this is so because the stick-slip movement of the base induces a whip effect that increases the response of the upper parts of the flexible bodies. Regarding the response of plate 3 the free-to-slide model, it is observed that when its acceleration drops to near zero, the plate vibrates seemingly similar to the low-amplitude vibrations produced by the sliding of the model base, although it occurs few seconds later, as if it were a reverberation of these base vibrations.

The response of the model in terms of accelerations, velocities and permanent displacements is shown in Figure 7, for a 1.2 sec time-window (from 10.2 to 11.3 sec). The model base displacements were monitored using a linear displacement transducer (see Figure 1), and the velocities and accelerations by means of the accelerometers laid down as shown in Figure 1.

The displacements time series of the model base (Figure 7a) shows periods where the body slides backwards (line inclined with positive slope), then there is a time span where it remains still (horizontal line) to slide forwards (line with negative slope) until it practically recuperates the backward displacement. Since the sliding surface is horizontal and the excitation remains constant, the net displacement when the shaking stops, is for all practical purposes equal to zero.

The velocity time histories recorded on the sliding surface and the base of the model are plotted in Figure 7b. These two curves hold the key information regarding the pattern of displacements endured by the free-to-slide base model. When the curves cross each other either the body starts sliding or comes to a stand still. Whenever these traces coincide, the body moves with the sliding table as if it were welded to it. Accordingly, as the body moves backwards (with respect to the sliding surface) its velocity is lower than that of the input (shaking table). The opposite is true whenever the body moves forwards. The body remains still if the velocities are equal.

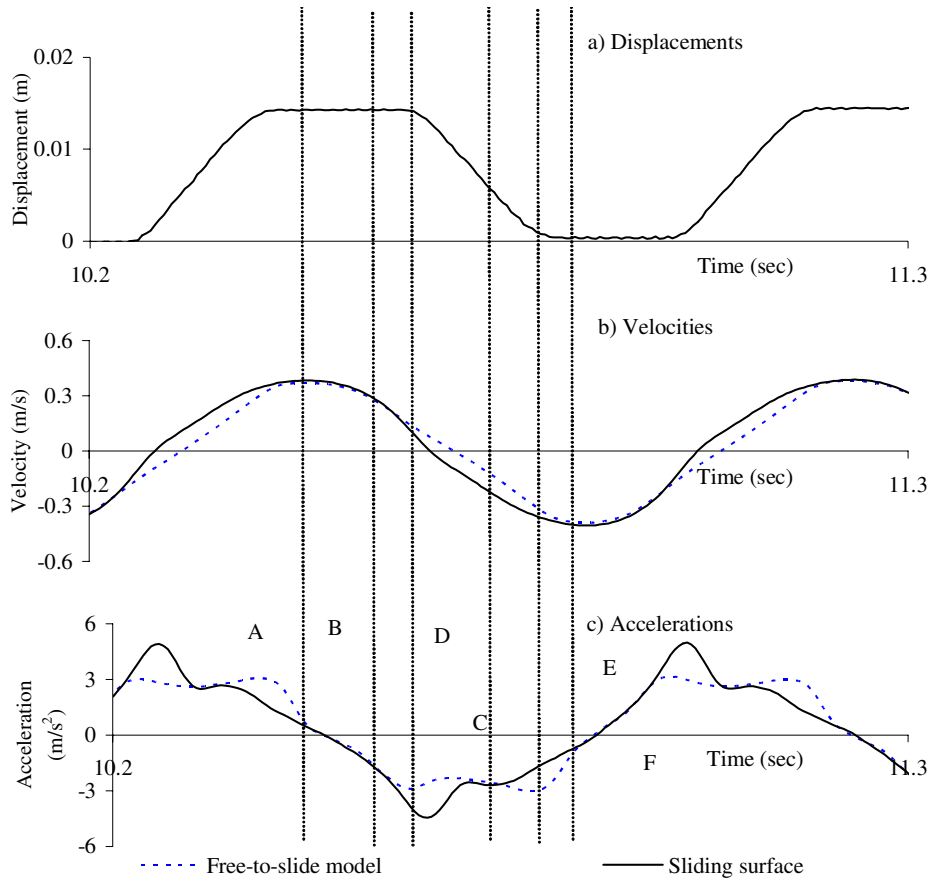


Figure 7. Acceleration, velocity and displacement on the base of the free-to-slide model

The accelerograms depicted in Figure 7c show the moment when the yield acceleration is reached, setting off the sliding of the flexible body. They also indicate that the body displacement continues despite the input acceleration dropping below the yield acceleration. This is due to a drop in the magnitude of static friction (friction developed before body sliding) to that of the kinetic friction, and also on account of the inertia the body has acquired. The body motion stops when the kinetic energy is dissipated (see point A in Figure 7c). Notice that at this moment the relative velocity of the body with respect to the sliding table is null. Again, when the yield acceleration (point B) is exceeded sliding begins and the movement pattern repeats itself.

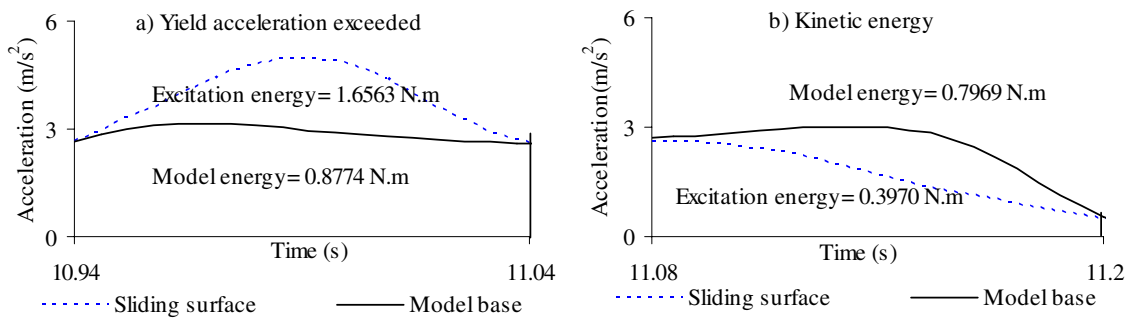


Figure 8. Energy transmission during the body displacement

Throughout the time spans when the body slides, the actual excitation differs to that provided by the input motion. When the body slides a cause of the yield acceleration being exceeded, the actual energy transmitted to the sliding body is lower than that of the input motion as shown in Figure 8a. This result shows that despite the excitation endured by the body decreases, it keeps on sliding. This confirms what was stated before, regarding a decrease in the friction developed at the interface body-sliding surface. Accordingly, the assumption that is usually made to compute permanent displacements, that implies that the input motion is not modified when sliding occurs is contradicted by the results of Figure 8a. Regarding the displacements caused by the kinetic energy acquired by the body, in Figure 8b it is shown that the body energy is higher than the energy contained by the input motion. This backs up the statement in the sense that the body keeps on sliding until the kinetic energy is dissipated. When it is fully dissipated, the body comes to a stand still with respect to the sliding surface.

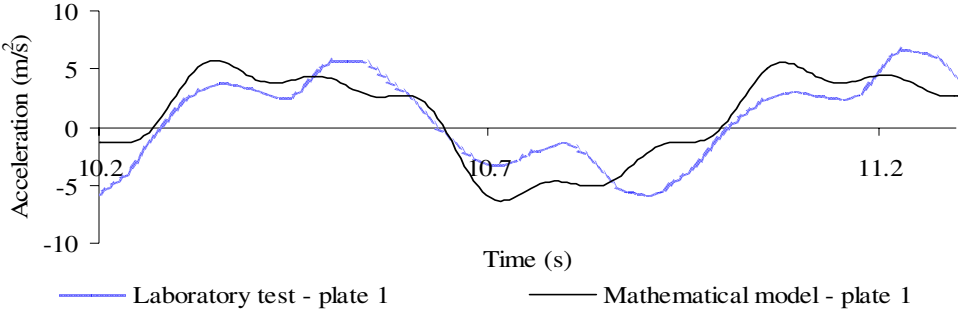


Figure 9. Comparison between mathematical model and laboratory results with fixed system

Figures 9 and 10 show comparisons between the responses measured and those computed with the analytical model included in this paper. Both free-to-slide and fixed-base models are considered. The results show that the general patterns of the accelerograms are fairly reproduced, although some important differences show up, particularly when sliding due to the kinetic effect occurs. These discrepancies may be due to the dynamic (kinetic) friction adopted (constant) in the analysis. It is known (Constantinou [13] and Rajagolapan [14]) that the magnitude of the kinetic friction is affected (for a given material) by the sliding velocity rate and the amount of accumulated displacements. With respect to the displacements (Figure 11), the model yields results closer to the experimental values.

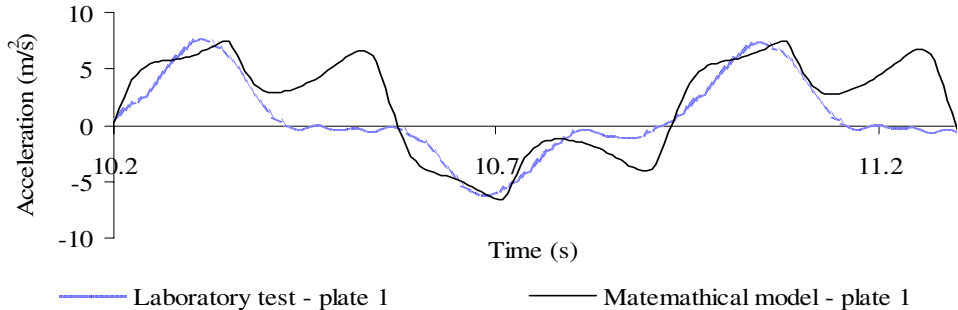


Figure 10. Comparison between mathematical model and laboratory results with free-to-slide system

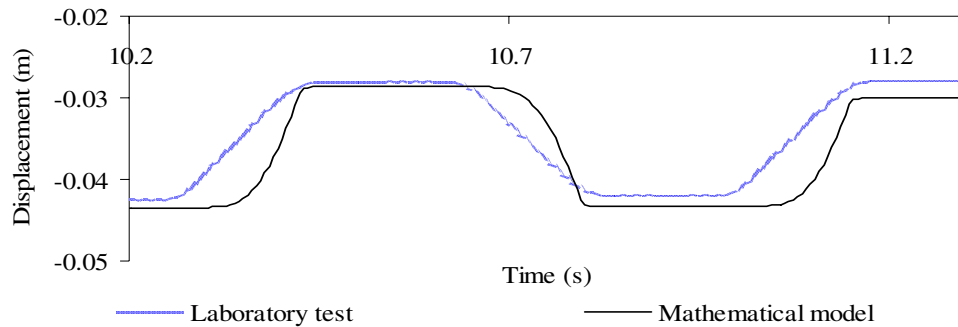


Figure 11. Comparison between mathematical model and laboratory results with free-to-slide system

## CONCLUSIONS

On the bases of the results included in this paper it may be argued that the dynamic characteristics of the system, friction parameters, input motion, kinetic effects and variation of the energy transmitted across the body-sliding surface interface greatly influence the response of systems with free-to-slide and fixed-base boundary conditions. Accordingly, methods based on the rigid wedge approach (Newmark's) are an oversimplification of the physical phenomenon.

These aspects were observed, analyzed and verified through the laboratory tests realized. The system behavior endures important changes when the flexible body slides over the shaking table (sliding surface). Thus, it is necessary to account for the ensuing effects in the analytical model, as it is intended in the method advanced in this paper.

## REFERENCES

1. Newmark N. M. (1965). "Effects of Earthquakes on Dams and Embankments." *Geotechnique* 15(2): 139-160.
2. Ambraseys, N. N. (1972). "Behavior of Foundation Material During Strong Earthquakes." *Proceedings of the Fourth European Symposium on Earthquake Engineering, London, Vol 7.*
3. Makdisi, F. I. and Seed, H. B. (1978). "Simplified Procedure for Estimating Dam and Embankment Earthquake-Induced Deformations." *Journal of Geotechnical Engineering. ASCE*, 104 (7), 849-867.
4. Chopra, A. K. and Zhang, L. (1991). "Earthquake-Induced Base Sliding of Concrete Gravity Dams." *Journal of Structural Engineering. ASCE*, 117 (12), 3698-3719.
5. Kramer, S. L. and Smith, M. W. (1997). "Modified Newmark Model for Seismic Displacements of the Compliant Slopes." *Journal of Geotechnical Engineering. ASCE*, 123 (7), 635-644.
6. Rathje, E. M and Bray, J. D. (2000). "Nonlinear Coupled Seismic Analysis of Earth Structures." *Journal of Geotechnical and Geoenvironmental Engineering. ASCE*, 2000; 126 (11): 1002-1014.
7. Botero E. and Romo M. P. (2002). "A Two Dimensional Procedure for Slopes Seismic Analysis." *12th European Conference on Earthquake Engineering. London, paper 053.*
8. Botero E. and Romo M. P. (2003a). "Analysis Method for Translational Failures in Slopes." *12<sup>th</sup> Panamerican Conference on Soil Mechanics and Geotechnical Engineering. Cambridge.*
9. Botero E. and Romo M. P. (2003b). "Seismic Analysis of Slope Stability." *Geofisica Internacional*. 42 (2), 219-225.
10. Botero E, and Romo M. P. (2001). "Seismic Analyses of Slopes." *Fifteen International Conference on Soil Mechanics and Geotechnical Engineering. Istanbul, Turkey. 1091-1094.*

11. Botero E. (2004) "Modelo Bidimensional no Lineal para el Análisis del Comportamiento Dinámico de Estructuras Terreas." Phd Thesis (in Spanish).
12. Houston S. L., Houston W. N. and Padilla J. M. (1987). "Microcomputer-aided Evaluation of Earthquake-Induced Permanent Slope Deformation." *Journal of Microcomputers in Civil Engineering*. 2(3), 207-222.
13. Constantinou M. and Mokha A. (1990). "Teflon Bearings in Base Isolation. II: Modelling." *Journal of Structural Engineering*. Vol. 116, No 2.
14. Rajagolapan S. and Prakash V. (2001). "An Experimental Method to Study High Speed Sliding Characteristics During Forward and Reverse Slip." *Wear*. Vol. 249 (8), 687-701.